A Multireader Exploratory Evaluation of Individual Pulse Sequence Cancer Detection on Prostate Multiparametric Magnetic Resonance Imaging (MRI)

Sonia Gaur, BS[1], Stephanie Harmon, PhD[1], Rajan T. Gupta, MD, Daniel J. Margolis, MD, Nathan Lay, PhD, Sherif Mehralivand, MD, Maria J. Merino, MD, Bradford J. Wood, MD, Peter A. Pinto, MD, Joanna H. Shih, PhD, Peter L. Choyke, MD, Baris Turkbey, MD

Abbreviations

mpMRI Multiparametric magnetic resonance imaging

T2W T2-weighted

DWI Diffusion-weighted imaging

DCE Dynamic contrast-enhanced

PI-RADSv2 Prostate Imaging-Reporting and Data System version 2

WP Whole prostate

TZ Transition zone

PZ Peripheral zone

PSA Prostate-specific antigen

ADC Apparent diffusion coefficient

Rationale and Objectives: To determine independent contribution of each prostate multiparametric magnetic resonance imaging (mpMRI) sequence to cancer detection when read in isolation.

Materials and Methods: Prostate mpMRI at 3-Tesla with endorectal coil from 45 patients ($n = 30$ prostatectomy cases, $n = 15$ controls with negative magnetic resonance imaging [MRI] or biopsy) were retrospectively interpreted. Sequences (T2-weighted [T2W] MRI, diffusion-weighted imaging [DWI], and dynamic contrast-enhanced [DCE] MRI; $N = 135$) were separately distributed to three radiologists at different institutions. Readers evaluated each sequence blinded to other mpMRI sequences. Findings were correlated to whole-mount pathology. Cancer detection sensitivity, positive predictive value for whole prostate (WP), transition zone, and peripheral zone were evaluated per sequence by reader, with reader concordance measured by index of specific agreement. Cancer detection rates (CDRs) were calculated for combinations of independently read sequences.

Results: 44 patients were evaluable (cases median prostate-specific antigen 6.83 [range 1.95−51.13] ng/mL, age 62 [45−71] years; controls prostate-specific antigen 6.85 [2.4−10.87] ng/mL, age 65.5 [47−71] years). Readers had highest sensitivity on DWI (59%) vs T2W MRI (48%) and DCE (23%) in WP. DWI-only positivity (DWI+/T2W−/DCE−) achieved highest CDR in WP (38%), compared to T2W-only (CDR 24%) and DCE-only (CDR 8%). DWI+/T2W+/DCE− achieved CDR 80%, an added benefit of 56.4% from T2W-only and of 42% from DWI-only ($P < .0001$). All three sequences interpreted independently positive gave highest CDR of 90%. Reader agreement was moderate (index of specific agreement: T2W = 54%, DWI = 58%, DCE = 33%).

Conclusions: When prostate mpMRI sequences are interpreted independently by multiple observers, DWI achieves highest sensitivity and CDR in transition zone and peripheral zone. T2W and DCE MRI both add value to detection; mpMRI achieves highest detection sensitivity when all three mpMRI sequences are positive.

Key Words: Multiparametric; MRI; prostate; sequence; PI-RADSv2.

Published by Elsevier Inc. on behalf of The Association of University Radiologists.

Acad Radiol 2019; 26:5−14

From the Molecular Imaging Program, National Cancer Institute, National Institutes of Health, 10 Center Drive, Room B3B85, Bethesda, MD 20814 (S.G., P.L.C., B.T.); Clinical Research Directorate/Clinical Monitoring Research Program, Leidos Biomedical Research, Inc., National Cancer Institute, Frederick, Maryland (S.H.); Duke University Medical Center, Duke Cancer Institute, Durham, North Carolina (R.T.G.); Weill Cornell Imaging, New York-Presbytarian Hospital, New York, New York (D.J.M.); Computer-Aided Diagnosis Laboratory, Clinical Center, National Institutes of Health, Bethesda, Maryland (N.L.); Urologic Oncology Branch, National Cancer Institute, National Institutes of Health, Bethesda, Maryland (S.M., P.A.P.); Department of Pathology, National Cancer Institute, National Institutes of Health, Bethesda, Maryland (M.J.M.); Center for Interventional Oncology, Clinical Center, National Institutes of Health, Bethesda, Maryland (B.J.W.); Biometric Research Branch, National Cancer Institute, National Institutes of Health, Rockville, Maryland (J.H.S.). Received January 7, 2018; revised March 19, 2018; accepted March 24, 2018.
Address correspondence to: B.T. e-mail: turkbeyi@mail.nih.gov
[1] Both authors contributed equally to this work.

Published by Elsevier Inc. on behalf of The Association of University Radiologists.
https://doi.org/10.1016/j.acra.2018.03.024

ISA
Index of specific agreement
CDR
Cancer detection rate

INTRODUCTION

Prostate multiparametric magnetic resonance imaging (mpMRI) has become an established method for localizing clinically significant prostate cancer and for informing subsequent treatment planning decisions (1–3). The technique combines anatomical data from T2-weighted (T2W) magnetic resonance imaging (MRI) with functional data from diffusion-weighted imaging (DWI) and dynamic contrast-enhanced (DCE) MRI to provide up to 90% reported sensitivity in detection of significant disease (4). mpMRI interpretation inherently relies on findings across multiple sequence images; however, the degree to which each pulse sequence contributes to overall detection sensitivity remains unclear.

Perception of the contribution of each pulse sequence has evolved. Initial Prostate Imaging-Reporting and Data System (PI-RADS) guidelines for standardization of prostate MRI interpretation assumed equal diagnostic weight for each of the three sequences; whereas the current PI-RADS version 2 (PI-RADSv2) has weighted sequences differently depending on the lesion location within the prostate (5). The change was based on expert consensus and zone-focused data reflecting possibly optimal cancer detection in the transition zone (TZ) from T2W MRI sequences and in the peripheral zone (PZ) from DWI sequences (6–9). However, these studies, along with recent PI-RADSv2 validations, are almost always based on mpMRI evaluations using complete mpMRI sets (10–13). In this context, conclusions about the value of individual sequences in cancer detection are subject to innate reader bias as each sequence validates the other in the reader's mind. Moreover, such studies are often based on a single institution's experience. As a result, there is continued uncertainty about the true value of each mpMRI sequence in cancer detection. Therefore, the purpose of this work was to determine the independent contribution of each prostate mpMRI sequence to cancer detection when read in isolation.

MATERIALS AND METHODS

Study Population

This Health Insurance Portability and Accountability Act-compliant retrospective evaluation of prospectively acquired data was approved by local ethics committee. Written informed consent was given by all patients. Flow diagram illustrating patient exclusion and inclusion is given in Figure 1. All patients underwent complete mpMRI (T2W MRI, DWI [apparent diffusion coefficient {ADC} map, *b*-2000 DWI acquisition], and DCE MRI) at 3-Tesla with endorectal coil performed at one institution. In population of consecutive patients imaged between April 2012 and June 2015 considered for inclusion, 179 underwent radical prostatectomy and 92 had no lesions detected on mpMRI and subsequent negative 12-core systematic biopsy guided by mpMRI-transrectal ultrasound fusion technique using the Uronav platform. Patients were excluded for receiving any prior treatment and for having artifacts arising from hip prostheses, or if acquired

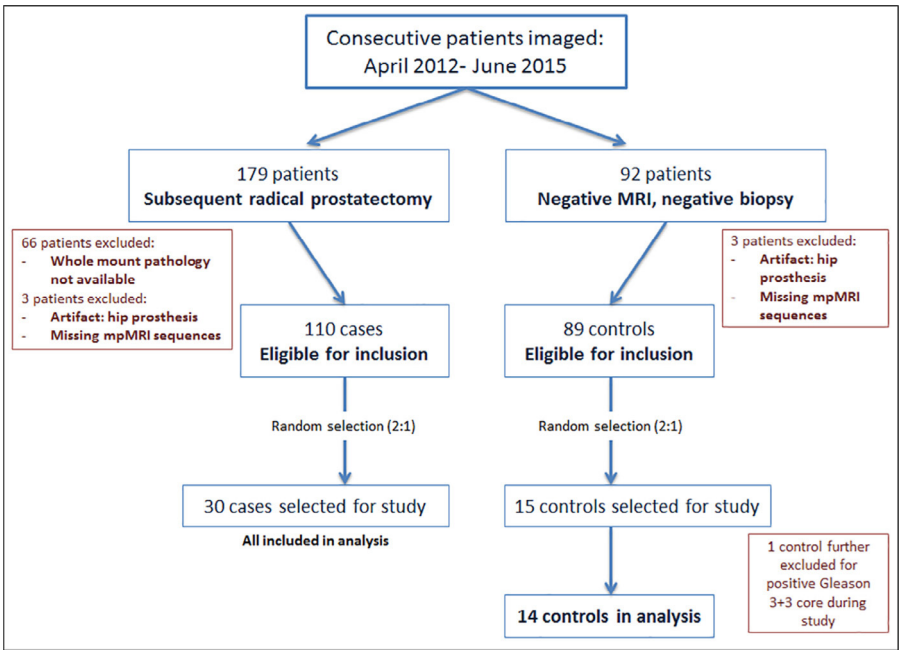

Figure 1. Study design. Flow diagram shows exclusion criteria as well as random selection of patients for inclusion in study. MRI, magnetic resonance imaging; mpMRI, multiparametric MRI. (Color version of figure is available online.)

mpMRI was missing any sequences. Cases were additionally excluded if whole-mount specimen mapping with lesion-specific Gleason scores was not available (total exclusions $n = 69$ cases, $n = 3$ controls). From remaining eligible patients, 45 ($n = 30$ cases, $n = 15$ controls) were randomly selected in a two:one ratio of cases:controls for study inclusion. Indications for imaging included rising prostate-specific antigen (PSA) with prior negative biopsy ($n = 12$ controls), high measured PSA without prior biopsy ($n = 3$ controls), referral for fusion-guided biopsy and cancer staging ($n = 29$ cases), and referral for cancer staging after a positive biopsy ($n = 1$ case). Patients originally presented to the National Institutes of Health as part of accrual for an approved prostate cancer protocol.

Study Design

As this method of studying independent sequence cancer detection did not suggest an ideal set point for facilitating statistical powering, the study was conducted as a small pilot study and the sample size utilized reflects its exploratory purpose. The patient population is a subset of patients from a larger ongoing multireader study of a computer-aided diagnosis system.

Three radiologists participated as readers. All were from different institutions, highly experienced in prostate mpMRI (>2000 cases each in the last 2 years), and familiar with reading endorectal coil mpMRI. The readers were blinded to clinical and pathologic data while conducting reads. The readers were asked to independently evaluate each sequence in the following manner:

Each complete mpMRI data per patient were split into three individual MRI sequences and separately anonymized within the following groupings: T2W MRI (axial and sagittal sets), DWI (ADC map and *b*-2000 DWI sets), and DCE MRI (raw data of time points at each slice location). The resultant 135 anonymized pulse sequence datasets were randomly ordered and distributed to readers for interpretation.

MRI Technique

All magnetic resonance images were acquired at 3-Tesla (Achieva 3.0T-TX, Phillips Healthcare, Best, Netherlands) using an endorectal coil (BPX-30, Medrad, Pittsburgh, PA) filled with 45-mL perfluorocarbon-based fluid (Fluorinert, 3M, Maplewood, MN) and anterior half of a 32-channel cardiac SENSE coil (InVivo, Gainesville, FL). All patients underwent complete mpMRI protocol, which consisted of the following sequences: T2W MRI (axial, coronal, sagittal), DWI (ADC map calculated from five evenly spaced *b*-values between $0-750\ s/mm^2$ and an acquired high *b*-value image of *b*-$2000\ s/mm^2$), and DCE MRI. Full mpMRI parameters are given in Table 1.

MRI Interpretation

Readers were instructed to use RadiAnt DICOM Viewer to view images (14). All 135 sequences were randomized per reader and provided in this order with a read-out form designed with Microsoft Access (15). Within this programmed form, shown in Figure 2, readers recorded up to four detected lesions per sequence. Readers identified suspicious regions on each sequence utilizing visual patterns characteristic for tumor as outlined in PI-RADSv2 (5). For each lesion detected, readers recorded lesion location (zone and side of prostate), annotated the provided MRI sequence to delineate the diameter of the identified lesion, and uploaded a screenshot. All data were recorded in a linked Microsoft Access database.

Pathology Correlation

After mpMRI, case patients underwent robotic-assisted radical prostatectomy. For optimal image-pathology correlation, all prostate specimens were processed with patient-specific MRI-based three-dimensional printed molds with sections

TABLE 1. Multiparametric MRI Acquisition Parameters Given for Prostate Imaging at 3-Tesla (3T) with Use of an Endorectal Coil.

Multiparametric MRI Sequence Parameters at 3T

Parameter	T2-Weighted	DWI*	High *b*-Value DWI†	DCE MRI‡
Field of view (mm)	140 × 140	140 × 140	140 × 140	262 × 262
Acquisition Matrix	304 × 234	112 × 109	76 × 78	188 × 96
Repetition time (ms)	4434	4986	6987	3.7
Echo time (ms)	120	54	52	2.3
Flip angle (degrees)	90	90	90	8.5
Section thickness (mm), no gaps	3	3	3	3
Image reconstruction matrix (pixels)	512 × 512	256 × 256	256 × 256	256 × 256
Reconstruction voxel imaging resolution (mm/pixel)	0.27 × 0.27 × 3.00	0.55 × 0.55 × 2.73	0.55 × 0.55 × 2.73	1.02 × 1.02 × 3.00
Time for acquisition (min:s)	2:48	4:54	3:50	5:16

Sequences acquired include T2-weighted, diffusion-weighted imaging (DWI) that includes apparent diffusion coefficient map calculation, and a high *b*-value sequence, and dynamic contrast enhanced (DCE) magnetic resonance imaging (MRI).

* For ADC map calculation. Five evenly spaced *b*-values ($0-750\ s/mm^2$) were used.

† $b = 2000\ s/mm^2$.

‡ DCE MRI obtained before, during, and after a single dose of gadopentetate dimeglumine 0.1 mmol/kg at 3 mL/s. Each sequence was obtained at 5.6 s intervals.

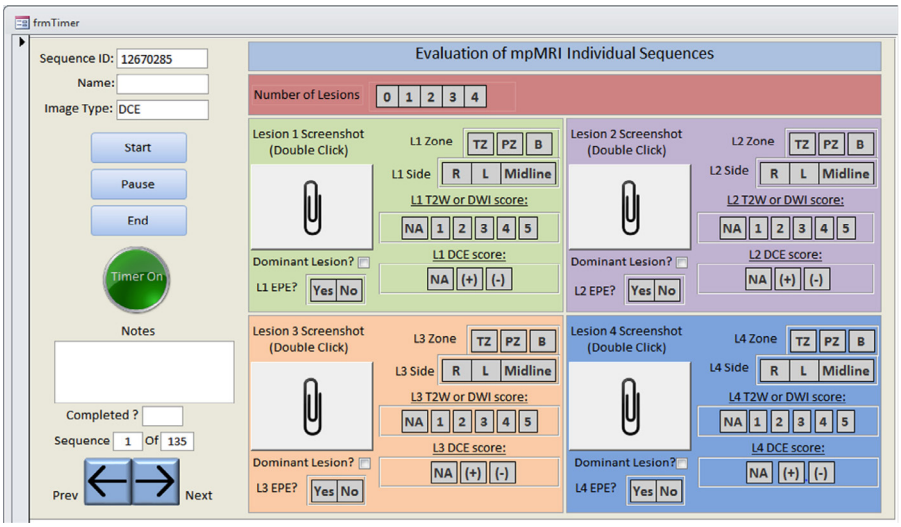

Figure 2. Reader data collection. Microsoft Access-designed application used to collect data from each reader. All patient sequence IDs and names are anonymized, and all 135 sequences appeared in random order to the reader. Readers could identify up to four lesions per sequence, and gave lesion information using form buttons. Each lesion's *paperclip box* represents where the reader would attach each lesion screenshot. B, both zones; DCE, dynamic contrast-enhanced; DWI, diffusion-weighted imaging; EPE, extraprostatic extension; L, left; NA, not applicable; PZ, peripheral zone; R, right; T2W, T2-weighted; TZ, transition zone. (Color version of figure is available online.)

cut spanning apex to base (16). One highly experienced genitourinary pathologist annotated the location of cancerous regions and lesion-specific Gleason scores ($\geq 3+3$) were assigned. A prostate mpMRI-focused research fellow performed radiologic-pathologic correlation using screenshot annotations of detected lesions from each reader. Magnetic resonance lesions detected were correlated to the pathology maps using visible prostate landmarks and lesion morphology. Lesions outlined on pathology but not detected by any readers were noted as false negative reads in subsequent analysis.

Statistical Analysis

Lesions were considered detected by a reader if a screenshot was uploaded showing clear annotation of the lesion on the sequence, with a category assigned. Reader-based lesion detection sensitivity was evaluated for each sequence. Concordance of lesion detection across readers was measured by index of specific agreement (ISA), defined as the conditional probability of a randomly selected individual reader, detecting a lesion in the same location as a blinded, independent reader. Pairwise ISAs were calculated over three pairs of readers and average ISA was reported. Cancer detection rate (CDR) was defined as the proportion of true positive lesions among all detected lesions (sum of true positives and false positives) and was calculated as the weighted average of reader CDRs. For example, a single unique lesion detected by all readers would be considered as three total lesions. This weighted average serves to minimize the variability of CDRs in categories where the number of lesions was small. All detected lesions were classified based on independent positivity read from all three sequences, lending to seven possible combinations of sequence detection positivity for each reader: T2W+/DWI−/DCE− (T2W-only), T2W−/DWI+/DCE− (DWI-only), T2W−/DWI−/DCE+ (DCE-only), T2W+/DWI+/DCE− (T2W+ DWI+), T2W+/DWI−/DCE+ (T2W+ DCE+), T2W−/DWI+/DCE+ (DWI+ DCE+), and T2W+/DWI+/DCE+ (all positive). Sensitivity and CDR are reported for whole prostate (WP), TZ, and PZ, separately.

Standard errors and 95% confidence intervals were estimated from 2000 bootstrap samples by random sampling on the patient-level to account for intrapatient correlation arising from multiple-readers, multiple lesions, and multiple sequences. Proportion of case and control patients were maintained in the bootstrap resampling procedure. The 95% confidence limits were taken from the 2.5% and 97.5% percentiles of the bootstrap distribution, and the Wald test was used to test the difference in CDRs across combinations of sequence positivity. All P values correspond to two-sided tests, with a P value $<.05$ considered to represent a significant difference.

RESULTS

Patient and Lesion Characteristics

The final study population consisted of 44 patients. One control patient was excluded after positive biopsy result (Gleason 3 + 3) following initial inclusion. Median age for cases and controls was 62 (range 45−71) and 65.5 (47−71) years, respectively, and median PSA for cases and controls was 6.83 (range 1.95−51.13) and 6.85 (2.4−10.87) ng/mL. Median time between MRI and radical prostatectomy was 3 (range 0.67−13) months for case patients. For control patients, median time between MRI and negative biopsy was 37.1 (0.07−104.2) months.

A total of 232 unique lesions were detected across all three readers on all individual sequences, of which 128 of 232 were PZ lesions (55.1%), 103 of 232 were TZ lesions (44.4%), and one lesion spanned both zones. Histopathologically, 30.2% of identified lesions (70 of 232 lesions) were tumor-positive. Mean histologic lesion size was 7.2 (0.1−271.7) mL. Of these 70 lesions, 57, 10, 2, and 1 were Gleason 3 + 4, 4 + 4, 4 + 5, and 5 + 4, respectively.

Reader-based Individual Sequence Sensitivity and Agreement

Reader agreement was moderate for all sequences; ISA was highest for DWI at 58%, followed by T2W at 54%, and DCE

at 33% (Fig 3). Analysis of pairwise ISA showed higher concordance between Readers 1 and 2 for lesion detection on DCE (Table 2).

Lesion zonal breakdown with individual true positive detection, used for sensitivity analysis, is given in Table 3. For WP, reader sensitivity was highest with DWI (average 59%, range [51%–71%]), followed by T2W (48%, [39%–59%]), and then DCE (23%, [13%–36%]). This pattern remained consistent across zones, with DWI achieving highest average sensitivity of 50% in the PZ, and 69% in the TZ (Fig 4).

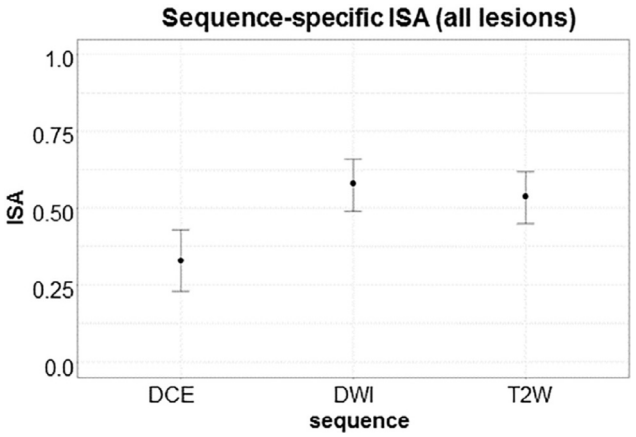

Figure 3. Inter-reader agreement. Average pairwise Index of Specific Agreement (ISA) evaluated for all identified lesions in the whole prostate is given for each sequence. DCE, dynamic contrast-enhanced; DWI, diffusion-weighted imaging; T2W, T2-weighted.

TABLE 2. Pairwise Inter-reader Specific Agreement (ISA) in the Whole Prostate. ISA Is Given for All Reader Combinations for Each Sequence Type

	Readers 1–2	Readers 1–3	Readers 2–3
T2W	0.51	0.55	0.56
DWI	0.59	0.59	0.57
DCE	0.46	0.24	0.30

Individual and Additive Value of MRI Sequences for Cancer Detection

As a single sequence, DWI showed highest individual CDR in WP, PZ, and TZ at 38%, 36%, and 40%, respectively. When DWI and T2W MRI independently identified the same lesion, CDR in WP, PZ, and TZ rose to 80%, 80%, and 81%, respectively. Highest CDR in the TZ was seen when the same lesion was identified independently on T2W and DCE (100% for $N = 4$ lesions). When the same lesion was independently identified on all three sequences, CDRs for WP, PZ, TZ were 90%, 85%, 94%, respectively (Fig 5). Examples of single sequence and independent identification on two sequences are shown in Figure 6.

Added benefit to CDR of each sequence combination (ΔCDR) is given in Table 4. Overall, in the WP, DWI was a significant addition to T2W-positive and DCE-positive lesions, adding 56.4% and 59% to the detection rates, respectively ($P < .0001$). Similarly, T2W positivity was a significant addition to DWI-positive lesions (42% increased CDR, $P < .0001$) and DCE-positive lesions (42.3% increased CDR, $P = .03$). Together, DWI was the most significant addition to lesions detected both on T2W and DCE independently, adding 40% to CDR ($P = .03$).

The effect of different combinations of independently interpreted pulse sequences on zone-based detection is given in Table 4. In the PZ, DWI consistently added the greatest benefit to positive T2W or DCE lesions ($P < .0001$ and $P < .01$, respectively) (Table 4). Only modest benefit was observed when a positive DCE lesion was also seen independently on T2W (16.3% CDR increase, $P = .38$, $N = 6$ lesions). In the TZ, the addition of DCE positivity added significant benefits to T2W-positive lesions (77.4% increased CDR, $P = .02$, $N = 4$ lesions). In cases in which lesions were detected by two independently positive sequences, no significant addition to detection was achieved by the addition of the third sequence in the TZ (Table 4).

DISCUSSION

It can be difficult to distinguish individual contribution of a pulse sequence in a multiparametric study when the study pulse sequences are viewed simultaneously, as the results of one

TABLE 3. Observed Number of True Positives for Each Reader, by Zone and within Each Sequence. Sensitivities Calculated for Figure 4 Were Derived From the Ratio of Number of True Positives to Number of Pathologically Confirmed Lesions (Condition True)

		Reader-detected True Positives								
		T2W			DWI			DCE		
Zone	Number of Pathologically Confirmed Lesions	R1	R2	R3	R1	R2	R3	R1	R2	R3
PZ	38	14	16	23	23	18	16	11	9	3
TZ	32	19	11	18	27	18	21	14	5	6
All	70	33	27	41	50	36	37	25	14	9

DCE, dynamic contrast-enhanced; DWI, diffusion-weighted imaging; PZ, peripheral zone; R, reader; T2W, T2-weighted; TZ, transition zone.

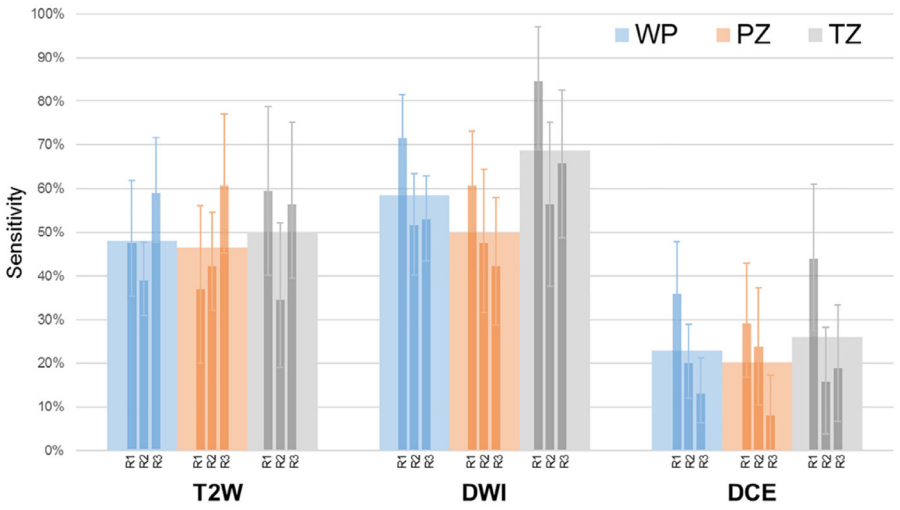

Figure 4. Reader-specific and average detection sensitivities per sequence. Reader detection sensitivity for T2-weighted (T2W), diffusion-weighted imaging (DWI), and dynamic contrast-enhanced (DCE) MRI sequences for whole prostate (WP), peripheral zone (PZ), and transition zone (TZ) lesions. Average across three readers is indicated by *wide solid bars* for WP, PZ, and TZ, with individual reader-based sensitivities and 95% confidence intervals overlaid as *narrower bars*. From *left* to *right*, the *narrow bars* indicate results for Reader 1 (R1), Reader 2 (R2), and Reader 3 (R3), respectively. True positive and condition positive findings from which these results were derived are available in Table 3. (Color version of figure is available online.)

sequence can bias the reader's opinion on other sequences. Such studies often conclude that DCE MRI adds little to mpMRI of the prostate**.** This study compares individual pulse sequences in a completely independent interpretation manner using different readers from different institutions, and suggests that when maximizing detection of prostate cancer with mpMRI, all sequences in mpMRI are contributory in an independent fashion. We found that although DWI consistently provided the highest sensitivity and independent CDR, this was closely matched by the sensitivity and CDR of T2W. DCE added moderate increases in CDR, and in some cases, these were quite significant when added to the findings of T2W and DWI. Our data suggest that identifying a dominant sequence or discounting the value of a certain sequence based on zone potentially reduces the impact of mpMRI.

DWI and T2W are generally considered key sequences for clinically significant cancer detection on mpMRI (12,17,18). The high predictive values reported for these two sequences are confirmed in this study, with both exhibiting relatively high reader sensitivity, ranging from 39% to 59% and 51% to 71%, respectively, across all readers. Additionally, both sequences significantly added to the CDR in combination with other sequences, suggesting that T2W and DWI are the two most essential sequences for maximizing cancer detection. We also report that of all three sequences, reader agreement was highest in T2W and DWI, indicating that readers are able to most commonly identify lesions on these two sequences. Although overall, reader agreement was moderate and prior studies have reported lesion detection agreement as high as 74%–93%, given the completely independent reads utilized in the present study in contrast to multiparametric application, the clinical scenarios cannot be reasonably compared (4).

Throughout the WP and by zones, DWI achieved the strongest performance for reader sensitivity and for additive value to other sequences. DWI characteristics are well known to be moderately inversely correlated with tumor Gleason score, and the association with likelihood of clinically significant disease is strongest in the PZ (19–23). These findings are also confirmed by our data, which show high sensitivity and detection in the PZ. In the TZ, DWI sequence interpretation is confounded by signal patterns from benign prostatic hyperplasia (24). However, DWI-positive lesions in the TZ achieved a CDR of 40% compared to T2W-positive lesions interpreted independently, which achieved a CDR of only 23%. This finding raises some questions regarding the "dominance" of T2W in the PZ and set forth in PI-RADSv2 (5). This is supported by other lines of evidence such as recent studies that have shown promise in using DWI signal difference to distinguish between tumor and benign tissue in the TZ, suggesting that perhaps DWI can play a more prominent role in detection of clinically significant cancer (21,25–27).

Some studies recommend dropping DCE altogether from mpMRI of the prostate (12,28–31). In PI-RADSv2, the role of DCE is minimized with readers simply evaluating for positive enhancement or lack of enhancement, and its role in determining overall PI-RADS categorization is limited to equivocal PZ lesions. In our analysis, reader detection on DCE, although inferior to T2W and DWI, nevertheless was contributory when read independently. In combination with other sequences, DCE added value to cancer detection, ranging from 9.6% to 28.3% in WP, 0.4% to 24.4% in PZ, and 13.3% to 77.4% in TZ. The small number of lesions that were positive on DCE, both alone and in combination with other sequences, limited the statistical power for evaluating its added benefit. However, the additional gain in CDR from DCE observed in this study suggests that excluding DCE MRI completely from the prostate mpMRI evaluation would compromise the efficacy of mpMRI.

Whereas the very first PI-RADS schema assumed equal diagnostic weight among all mpMRI sequences, the idea of a zone-based "dominant sequence" for optimal weighting was adopted in PI-RADSv2 (5,6). Initial studies validating PI-RADSv2 show some limitations in capturing optimal detection of clinically significant disease especially in PI-RADS "4" lesions (10,27,32). Further investigation has suggested that the zone-based weighting system is imperfect, with some

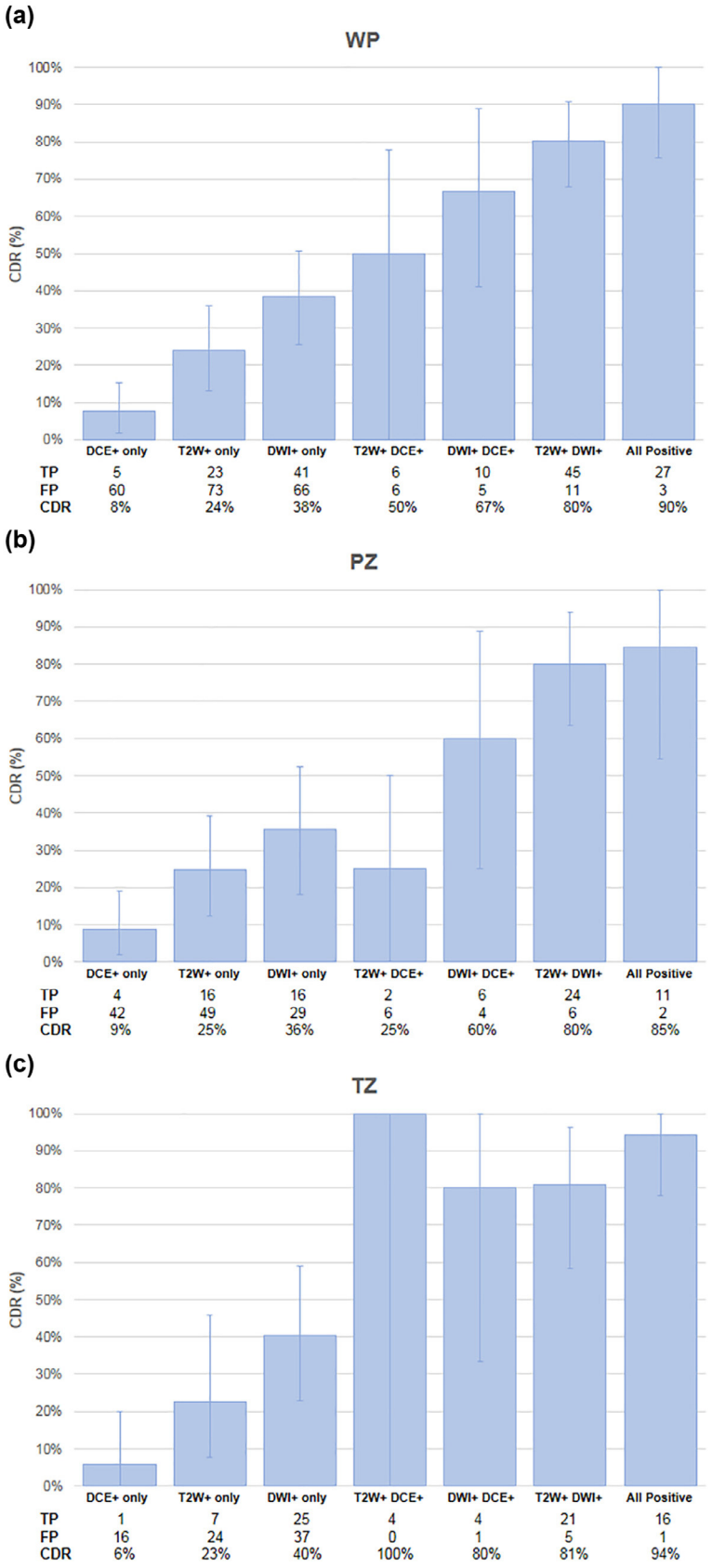

Figure 5. Cancer detection rates (CDRs) of sequence positivity combinations. CDRs in (**a**) whole prostate (WP), (**b**) peripheral zone (PZ), and (**c**) transition zone (TZ) for all seven combinations of sequence positivity, with 95% confidence intervals calculated from bootstrapping. Observed true positives (TPs), false positives (FPs), and CDRs are listed below each combination. Differences in CDR between combinations are presented in Table 4. DCE, dynamic contrast-enhanced; DWI, diffusion-weighted imaging; T2W, T2-weighted. (Color version of figure is available online.)

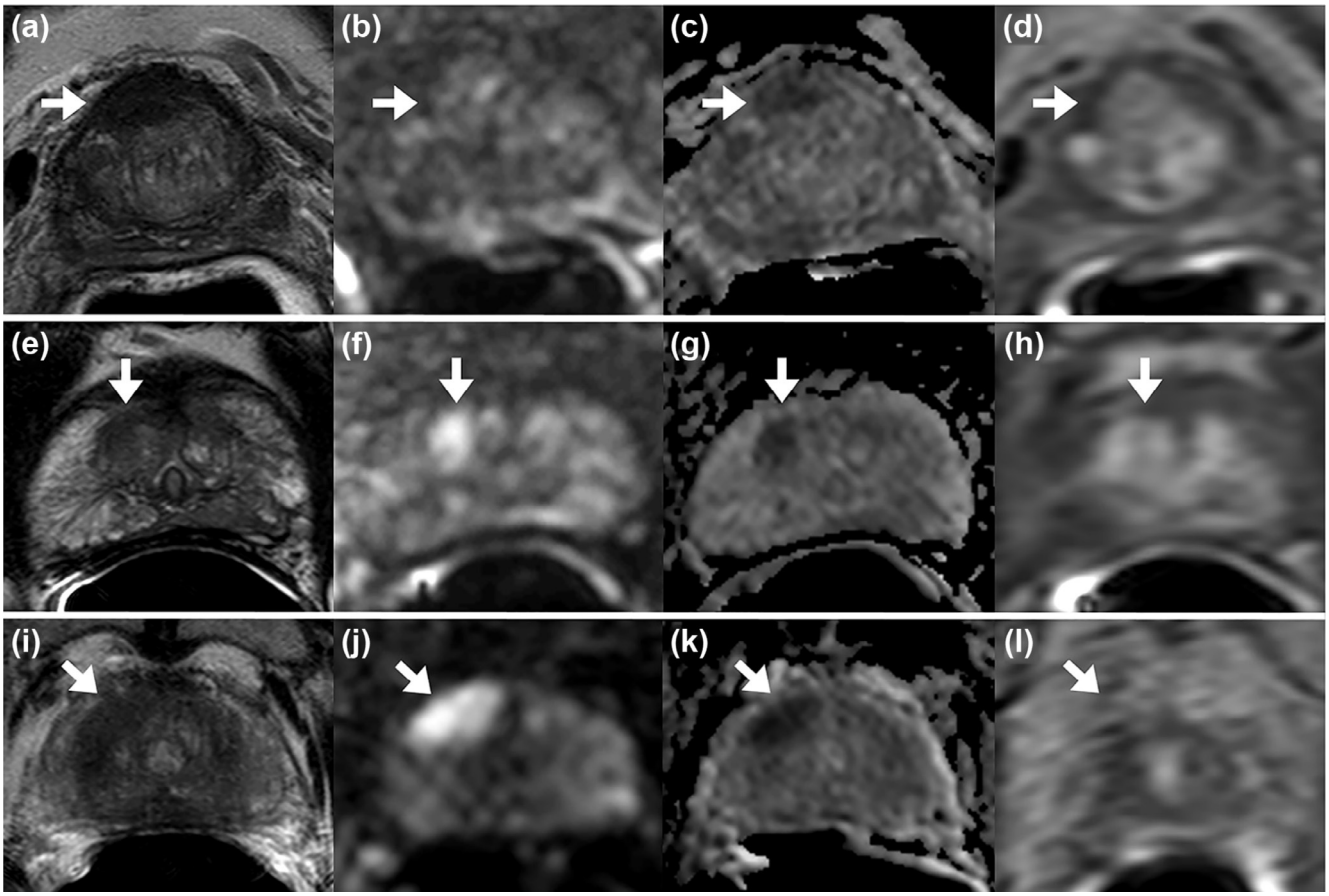

Figure 6. *Panels* (**a**–**d**): example T2-weighted (T2W)-only detection. A 58-year-old man with a serum prostate-specific antigen (PSA) of 7.09 ng/mL. All readers identified a lesion on axial T2W magnetic resonance imaging (MRI) that shows a hypointense lesion in the right anterior transition zone (*arrow,* **a**). Only one of three readers identified this lesion on diffusion imaging, including apparent diffusion coefficient (ADC) map (**b**) and *b*-2000 diffusion-weighted imaging (DWI, **c**). None of the readers detected this lesion on DCE (dynamic contrast-enhanced) MRI (**d**). The patient underwent radical prostatectomy and subsequent pathology mapping revealed Gleason 3 + 4 within this lesion. *Panels* (**e**–**h**): example DWI-only detection. A 51-year-old man with a serum PSA of 4.47 ng/mL. None of the readers reported findings on T2W MRI in this patient (**e**). All readers detected a lesion in the right apical anterior transition zone with restricted diffusion on ADC (**f**) and *b*-2000 (**g**) DWI. None of the readers detected this lesion on DCE MRI (**h**). The patient underwent radical prostatectomy and subsequent pathology mapping revealed Gleason 3 + 4 within this lesion. *Panels* (**i**–**l**): example T2W+/DWI+ detection. A 66-year-old man with serum PSA of 8.9 ng/mL. All readers reported a lesion on axial T2W MRI (**i**) in the right mid anterior transition zone. All readers additionally reported this lesion (*arrows*) on DWI, including ADC map (**j**) and *b*-2000 DWI (**k**). None of the readers detected this lesion on DCE MRI alone (**l**). Pathology mapping after radical prostatectomy revealed Gleason 3 + 4 within this lesion.

suggesting equal weighting of the three sequences had greater diagnostic performance than PI-RADSv2 in the PZ (33). Additionally, Rosenkrantz et al. found that assigning DWI more weight in the TZ than what is given in current PI-RADSv2 recommendations improved cancer detection (27). The data we have provided in this study suggest that there is likely no clear dominant sequence in each zone and further research remains to be done for designing the optimal weighting schema for prostate mpMRI interpretation.

As all pulse sequences were read independently, a false positive in one sequence would not add to overall false positivity by other sequences. The aim of this study was to elucidate detection and sensitivity of each sequence independently and without reader bias. However, the best way to truly assess combination detection and effect of each sequence on overall false positive rate would be to test all biparametric and triparametric combinations of imaging sequences in a prospective reading study, in addition to testing single sequence detection as is done here. Despite this, we have shown that false positive findings are lower in combinations of independent positivity, as demonstrated by higher CDR.

Our study has some limitations. First, our study cohort had only case patients who underwent subsequent radical prostatectomy and therefore harbored possibly higher grade cancers, leading to a selection bias compared to an average population of all patients undergoing mpMRI. Our definition for cancer was Gleason score $\geq 3 + 3$, and the randomly selected lesion population consisted of only Gleason 3 + 4 disease and above. We included control patients so as to reduce this effect. However, control populations are somewhat inherently limited by being only biopsy-proven since

TABLE 4. Cancer Detection Rate Benefit (ΔCDR) in Whole Prostate (WP), Peripheral Zone (PZ), and Transition Zone (TZ).

			WP			PZ			TZ		
Positive Sequence Combination	Baseline	Added	Baseline CDR	ΔCDR	*P* Value	Baseline CDR	ΔCDR	*P* value	Baseline CDR	ΔCDR	*P* Value
T2W+/DWI+/DCE−	T2W-only	DWI+	24.0%	56.4%	<0.0001	24.6%	55.4%	<0.0001	22.6%	58.2%	<0.0001
	DWI-only	T2W+	38.3%	42.0%	<0.0001	35.6%	44.4%	0.0002	40.3%	40.4%	0.0003
T2W+/DWI−/DCE+	DCE-only	T2W+	7.7%	42.3%	0.03	8.7%	16.3%	0.38	5.9%	94.1%	0.005
	T2W-only	DCE+	24.0%	26.0%	0.17	24.6%	0.4%	0.98	22.6%	77.4%	0.02
T2W−/DWI+/DCE+	DCE-only	DWI+	7.7%	59.0%	<0.0001	8.7%	51.3%	0.001	5.9%	74.1%	0.0005
	DWI-only	DCE+	38.3%	28.3%	0.03	35.6%	24.4%	0.16	40.3%	39.7%	0.09
T2W+/DWI+/DCE+	T2W+/DCE+	DWI+	50.0%	40.0%	0.03	25.0%	59.6%	0.002	100.0%	-5.9%	0.86
	DWI+/DCE+	T2W+	66.7%	23.3%	0.08	60.0%	24.6%	0.20	80.0%	14.1%	0.51
	T2W+/DWI+	DCE+	80.4%	9.6%	0.24	80.0%	4.6%	0.73	80.8%	13.3%	0.25

DCE, dynamic contrast-enhanced; DWI, diffusion-weighted imaging; T2W, T2-weighted.

ΔCDR is calculated as the difference in CDR between combinations of varying sequence positivity. Of note, CDRs for all sequence combinations are illustrated in Figure 5. For example, the baseline CDR for T2W-only in WP is 24.0% and the combined CDR for T2W+/DWI+ in WP is 80.4%, giving a ΔCDR (DWI benefit to T2W-only) of 56.4% $P < .0001$.

surgery cannot be offered to these patients. Additionally, as this was an exploratory evaluation with no set predicted detection rate for each sequence, the population used in this study was relatively small at 45 patients. Our results should be validated in a similar, optimally larger cohort. Moreover, this experimental read out study included three expert readers, but it may be more ideal to include readers with a greater diversity of experience. The readers' detection guidelines followed a framework outlined in PI-RADSv2 to optimize standardization across readers, but at the cost of standardization, perhaps detection instructions could be broadened to include in-house interpretation practices and central zone lesion identification.

CONCLUSIONS

In conclusion, when multiple observers independently read individual pulse sequences on prostate MRI, DWI achieves the highest cancer detection in both prostate zones; however, T2W and DCE MRI also add independent value to prostate cancer detection. These findings can serve as groundwork for future refinement of diagnostic criteria for mpMRI of the prostate.

ACKNOWLEDGMENTS

This project has been funded in whole or in part with federal funds from the National Cancer Institute, National Institutes of Health, under Contract No. HHSN261200800001E. The content of this publication does not necessarily reflect the views or policies of the Department of Health and Human Services, nor does mention of trade names, commercial products, or organizations imply endorsement by the U.S. Government.

The National Institutes of Health (NIH) Medical Research Scholars Program is a public-private partnership supported jointly by the NIH and generous contributions to the Foundation for the NIH from the Doris Duke Charitable Foundation, The American Association for Dental Research, the Colgate-Palmolive Company, Genentech and alumni of student research programs and other individual supporters via contributions to the Foundation for the National Institutes of Health.

REFERENCES

1. Siddiqui MM, Rais-Bahrami S, Turkbey B, et al. Comparison of MR/ultrasound fusion-guided biopsy with ultrasound-guided biopsy for the diagnosis of prostate cancer. JAMA 2015; 313:390–397.
2. Sciarra A, Barentsz J, Bjartell A, et al. Advances in magnetic resonance imaging: how they are changing the management of prostate cancer. Eur Urol 2011; 59:962–977.
3. Ahmed HU, Kirkham A, Arya M, et al. Is it time to consider a role for MRI before prostate biopsy? Nat Rev Clin Oncol 2009; 6:197–206.
4. Greer MD, Brown AM, Shih JH, et al. Accuracy and agreement of PIRADSv2 for prostate cancer mpMRI: a multireader study. J Magn Reson Imaging 2016; 45:579–585.
5. Weinreb JC, Barentsz JO, Choyke PL, et al. PI-RADS Prostate Imaging—Reporting and Data System: 2015, Version 2. Eur Urol 2016; 69:16–40.

6. Vache T, Bratan F, Mege-Lechevallier F, et al. Characterization of prostate lesions as benign or malignant at multiparametric MR imaging: comparison of three scoring systems in patients treated with radical prostatectomy. Radiology 2014; 272:446–455.
7. Akin O, Sala E, Moskowitz CS, et al. Transition zone prostate cancers: features, detection, localization, and staging at endorectal MR imaging. Radiology 2006; 239:784–792.
8. Hoeks CM, Hambrock T, Yakar D, et al. Transition zone prostate cancer: detection and localization with 3-T multiparametric MR imaging. Radiology 2013; 266:207–217.
9. Verma S, Rajesh A, Morales H, et al. Assessment of aggressiveness of prostate cancer: correlation of apparent diffusion coefficient with histologic grade after radical prostatectomy. AJR Am J Roentgenol 2011; 196:374–381.
10. Mertan FV, Greer MD, Shih JH, et al. Prospective evaluation of the prostate imaging reporting and data system version 2 for prostate cancer detection. J Urol 2016; 196:690–696.
11. Vargas HA, Hotker AM, Goldman DA, et al. Updated prostate imaging reporting and data system (PIRADS v2) recommendations for the detection of clinically significant prostate cancer using multiparametric MRI: critical evaluation using whole-mount pathology as standard of reference. Eur Radiol 2016; 26:1606–1612.
12. Junker D, Quentin M, Nagele U, et al. Evaluation of the PI-RADS scoring system for mpMRI of the prostate: a whole-mount step-section analysis. World J Urol 2015; 33:1023–1030.
13. Delongchamps NB, Rouanne M, Flam T, et al. Multiparametric magnetic resonance imaging for the detection and localization of prostate cancer: combination of T2-weighted, dynamic contrast-enhanced and diffusion-weighted imaging. BJU Int 2011; 107:1411–1418.
14. Medixant. RadiAnt DICOM Viewer. 2017.
15. Microsoft. Microsoft Access Professional Plus 2010. 2010.
16. Shah V, Pohida T, Turkbey B, et al. A method for correlating in vivo prostate magnetic resonance imaging and histopathology using individualized magnetic resonance-based molds. Rev Sci Instrum 2009; 80:104301.
17. Kwak JT, Sankineni S, Xu S, et al. Prostate cancer: a correlative study of multiparametric MR imaging and digital histopathology. Radiology 2017; 285:147–156.
18. De Visschere P, Lumen N, Ost P, et al. Dynamic contrast-enhanced imaging has limited added value over T2-weighted imaging and diffusion-weighted imaging when using PI-RADSv2 for diagnosis of clinically significant prostate cancer in patients with elevated PSA. Clin Radiol 2017; 72:23–32.
19. Wang XZ, Wang B, Gao ZQ, et al. Diffusion-weighted imaging of prostate cancer: correlation between apparent diffusion coefficient values and tumor proliferation. J Magn Reson Imaging 2009; 29:1360–1366.
20. Turkbey B, Shah VP, Pang Y, et al. Is apparent diffusion coefficient associated with clinical risk scores for prostate cancers that are visible on 3-T MR images? Radiology 2011; 258:488–495.
21. Tamada T, Sone T, Jo Y, et al. Apparent diffusion coefficient values in peripheral and transition zones of the prostate: comparison between normal and malignant prostatic tissues and correlation with histologic grade. J Magn Reson Imaging 2008; 28:720–726.
22. Hambrock T, Somford DM, Huisman HJ, et al. Relationship between apparent diffusion coefficients at 3.0-T MR imaging and Gleason grade in peripheral zone prostate cancer. Radiology 2011; 259:453–461.
23. Rosenkrantz AB, Parikh N, Kierans AS, et al. Prostate cancer detection using computed very high b-value diffusion-weighted imaging: how high should we go? Acad Radiol 2016; 23:704–711.
24. McNeal JE. Origin and evolution of benign prostatic enlargement. Invest Urol 1978; 15:340–345.
25. Xiaohang L, Bingni Z, Liangping Z, et al. Differentiation of prostate cancer and stromal hyperplasia in the transition zone with histogram analysis of the apparent diffusion coefficient. Acta Radiol 2017; 58: 1528–1534.
26. Kim CK, Park BK, Han JJ, et al. Diffusion-weighted imaging of the prostate at 3 T for differentiation of malignant and benign tissue in transition and peripheral zones: preliminary results. J Comput Assist Tomogr 2007; 31:449–454.
27. Rosenkrantz AB, Babb JS, Taneja SS, et al. Proposed adjustments to PI-RADS version 2 decision rules: impact on prostate cancer detection. Radiology 2017; 283:119–129.
28. Rud E, Baco E. Re: Jeffrey C. Weinreb, Jelle O. Barentsz, Peter L. Choyke, et al. PI-RADS Prostate Imaging—Reporting and Data System: 2015, Version 2. Eur Urol 2016;69:16–40: is contrast-enhanced magnetic resonance imaging really necessary when searching for prostate cancer? Eur Urol 2016; 70:e136.
29. Barentsz JO, Choyke PL, Cornud F, et al. Reply to Erik Rud and Eduard Baco's Letter to the Editor re: Re: Jeffrey C. Weinreb, Jelle O. Barentsz, Peter L. Choyke, et al. PI-RADS Prostate Imaging—Reporting and Data System: 2015, Version 2. Eur Urol 2016;69:16–40. Eur Urol 2016; 70: e137–e138.
30. Scialpi M, Prosperi E, D'Andrea A, et al. Biparametric versus multiparametric MRI with non-endorectal coil at 3T in the detection and localization of prostate cancer. Anticancer Res 2017; 37:1263–1271.
31. Stanzione A, Imbriaco M, Cocozza S, et al. Biparametric 3T magentic resonance imaging for prostatic cancer detection in a biopsy-naive patient population: a further improvement of PI-RADS v2? Eur J Radiol 2016; 85:2269–2274.
32. Mehralivand S, Bednarova S, Shih JH, et al. Prospective evaluation of prostate imaging-reporting and data system version 2 using the international society of urological pathology prostate cancer grade group system. J Urol 2017; 198:583–590.
33. Polanec S, Helbich TH, Bickel H, et al. Head-to-head comparison of PI-RADS v2 and PI-RADS v1. Eur J Radiol 2016; 85:1125–1131.